Vol 17 No 8, August 2008
1674-1056/2008/17(08)/3130-08

Chinese Physics B

© 2008 Chin. Phys. Soc.
and IOP Publishing Ltd

Observation of a diverse deviation from macropore-formation theory in silicon electrochemistry*

Bao Xiao-Qing(包晓清)[a)b)], Ge Dao-Han(葛道晗)[a)b)], and Jiao Ji-Wei(焦继伟)[a)†]

[a)] *State Key Laboratories of Transducer Technology, National Key Laboratories of Microsystem Technology, Shanghai Institute of Microsystem and Information, Chinese Academy of Sciences, Shanghai* 200050, *China*
[b)] *Graduate School of Chinese Academy of Sciences, Beijing* 100039, *China*

(Received 16 November 2007; revised manuscript received 14 March 2008)

Via anodizing patterned and unpatterned samples with a high HF concentration ([HF]), the degree of deviation from pore-formation theory was found to be markedly different. Based on the analysis of scanning electron microscope (SEM) micrographs and current–voltage ($I-V$) curves, the variation of physical and chemical parameters of patterned and unpatterned substrates was found to be crucial to the understanding of the observations. Our results indicate that the initial surface morphology of samples can have a considerable influence upon pore formation. The electric-field effect as well as current-burst-model was employed to interpret the underlying mechanism.

Keywords: space charge region, point nuclei, unpatterned specimen, $I-V$ curve
PACC: 8160, 8245, 8280

1. Introduction

Concerning pore silicon (PS) formation, numerous works with respect to space charge region (SCR) effects,[1−6] electrochemical oxidation,[7,8] hydrogen passivation,[9,10] avalanche breakdown,[11,12] diffusion-limited random walk,[13,14] surface instabilities,[15−17] current bursts,[18,19] geometry relativity,[20,21] solvent effects,[22] etc.[23−27] were advanced. Other reports established a framework in general for the pore-morphology under various conditions.[28−39]

In regard to macropore formation on n-type silicon, a marked deviation from SCR model was recently evidenced.[40,41] However, such a deviation has not been investigated in detail since to date relevant works focus primarily on the pore formation on linear nuclei.[40,41] To the best of our knowledge, on unpatterned samples or on samples pre-patterned with point nuclei, the detailed investigation of possible deviation from theory has not been carried out yet. A dissimilar deviation from the well-known SCR principles in patterned and unpatterned specimens, as shown in this work, can exist and can help us to further understand pore formation. The proper understanding of such phenomena can finally allow us to better control pore geometry (including both size and pitch of pores) and perhaps pore morphology (e.g., branching of pores), which could be potentially helpful for various applications, e.g., lithographic or non-lithographic photonic crystal fabrication.[33−41]

This work thus aims at photo-electrochemical etching of patterned and unpatterned n-type silicon with a high [HF]. Based on the comparison of pore formation in both cases (either pre-patterned or not pre-patterned), diverse deviations from the theory are observed and interpreted.

2. Experimental

Two kinds of samples based on n-type silicon (8–9 Ωcm, 450 μm-thick, CZ-grown, [100]-oriented and polished) were used: one kind was the blanket wafer (unpatterned sample) whereas the other kind was patterned with point defects as follows. A 500 nm-thick silicon nitride film was initially employed as a mask via PECVD (plasma-enhanced chemical vapour deposition). By standard photolithography, the specimen was textured with a hexagonal point-lattice of 3 μm lattice constant whereas the predefined points were of a square shape with a 1.5 μm side-length. After the removal (via ion beam bombardment) of silicon

*Project supported by the National High Technology Development Program of China (Grant No 2006AA04Z312) and the National Basic Research of China (Grant No 2006CB300403).
†Corresponding author. E-mail: jiaojw@mail.sim.ac.cn

nitride in the predefined area, defects shaped like inverted pyramids (point nuclei) were formed by TMAH (Tetramethylammonium hydroxide) etching to constitute the nucleation sites of pores. Finally, to generate comparability of data (with unpatterned samples), the remaining nitride on the patterned samples was removed by BOE (buffered oxide etchant), thus enabling a maskless and stable etching process.

All the specimens were anodized on an electrochemical etching platform in a decontamination chamber at room temperature. To efficiently evaluate the SCR effects, a fixed bias (18 V) was applied. A power-controlled halogen lamp (0–150 W) and an IR (infrared) filter was placed 12 and 3 cm, respectively, away from the back-side of the specimen to generate the electronic holes required for silicon dissolution; [1] and a platinum grid (served as cathode) was placed 5 mm away from the front side of specimen. An Au/Cr (300 nm/20 nm) film was sputtered on the backside of all specimens to establish a good ohmic contact, while an illumination window was formed via the removal of the corresponding Au/Cr layer by wet etching. Aqueous electrolytes were prepared based on a mixture of 48 wt.% hydrofluoric acid (HF) and deionized water; a few drops per litre of surfactant (NCW1001, WAKO) were added into the electrolytes.[42] The HF concentration was expressed by volume percentage of HF acid (but not pure hydrogen fluoride), unless otherwise stated. The pores produced were investigated with a field-emission scanning electron microscope (FESEM: Hitachi S-4700). Plan views show (100) plane, whereas after cleaving the samples, cross-sections show the pores in (011) or (110) cleavage planes.

3. Results

The dependence of pore morphology on HF concentration (abbreviated as [HF]) was investigated in detail. To clearly present the evolution of pore density with [HF], a fixed bias (18V) and a rather intensive illumination (140 W) were employed. For all [HF] (15%–40%) used in our experiments, a deviation from theory (SCR model) was found: since there was no inherent difference in the phenomena observed under different [HF] ($> 15\%$), the etching with 40% HF was chosen as an example. Firstly, via checking the behaviour of etching with unpatterned samples, an unambiguous reference was established (Fig.1). Then the anodization of samples patterned with point nuclei was performed (Fig.2).

In all cases, no pronounced current oscillations (if neglecting the weak oscillations with an approx. 0.1–1 $\mathrm{mA \cdot cm^{-2}}$ peak to peak amplitude) were observed; and at the start of each etching the current density increased quickly (within 40 seconds) to a high value which climbed up very slowly. Hence, the current density j observed for an unpatterned sample immediately after 5 minutes of etching was recorded (see the captions of Figs.1 and 2) for the estimation of pore-size. Note that after 5 minutes of etching, the pore growth and thus the current density will become sufficiently stable in our cases. It also should be noted that for an equal etching condition the j of patterned sample is much greater than that of unpatterned one as will be discussed later. If in light of the j ($72\,\mathrm{mA \cdot cm^{-2}}$) observed after 5 minutes of etching for the patterned sample, the theoretical pore-size ($4.56\,\mu$m) will be a little larger than but comparable to the corresponding value ($4.02\,\mu$m) shown in Table 1.

Table 1. Experimental data (Rows 1 and 2) showing a different deviation from theoretical data (Row 3).

	Diameter of stable pore/μm	Density of stable pore/$\mu\mathrm{m}^{-2}$	Growth rate/$\mu\mathrm{m \cdot min^{-1}}$
1. Unpatterned	1.5	0.08	4.6
2. Patterned	1	0.13	6.3
3. SCR Model	4.02	0.0035	20.8

The overall results obtained from experiments and SCR model are given in Table 1: the observations differ much from the theoretical data (calculated from the corresponding formulas given in Ref. [2]). Not least, if according to SCR model, the observed pore size, pore etch-rate and especially pore density should be nearly equal for the patterned and unpatterned samples, since the etching conditions (e.g., bias, illumination, electrolyte, etc., other than the initial morphology of sample surface) are identical. However, as shown in Table 1, the experimental results for patterned and unpatterned cases differ considerably

from each other. Therefore, the data observed for patterned and unpatterned samples exhibit different degrees of deviation from the theoretical value based on SCR model. Note that the unique difference between the two cases (see Figs.1 and 2) consists in the initial surface morphology, either pre-textured or untextured.

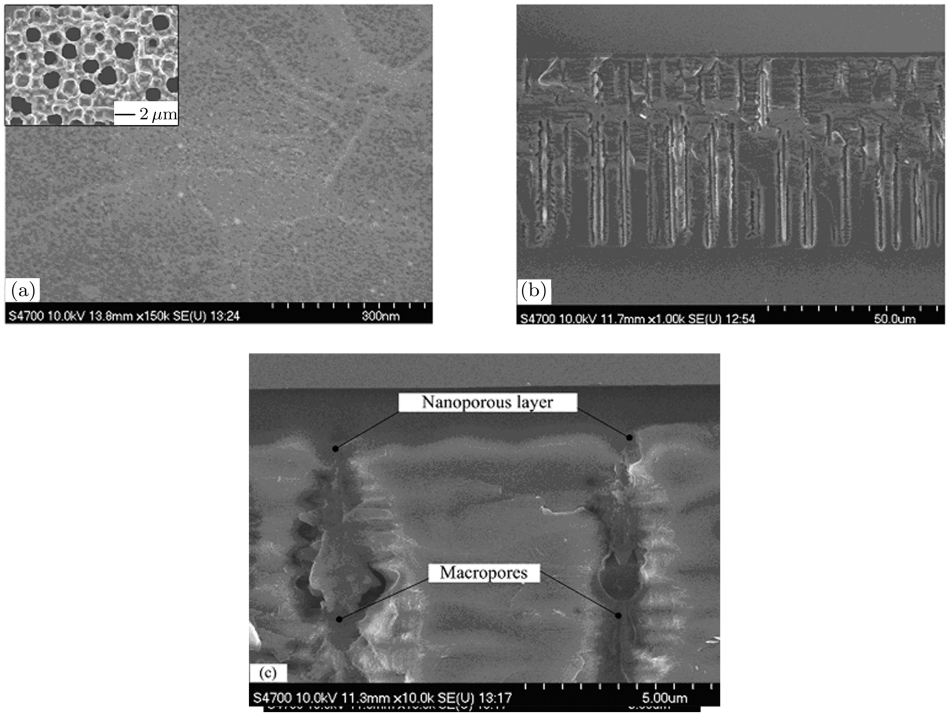


Fig.1. SEM micrographs: 40% HF, 140 W illumination, 18 V for 12 min, current density j (after 5 minutes of etching) $\approx 54\,\mathrm{mA/cm^2}$. (a) Plan view: the top diameters, i.e., the openings (the dark ones) of stable pores, can be estimated as ∼5–10 nm (but cannot be exactly identified since they are beyond the resolution of our equipment). Thus the inset shows the surface after removing the nanoporous layer via wet etching (25 wt% KOH for 3 min at room temperature $\sim 20^\circ$C): the density of stable pores can be estimated as $\sim 0.08\,\mu\mathrm{m}^{-2}$. (b) Cross-section (without removing the nanoporous layer via KOH etching): stable pores with $\sim 55\,\mu$m depths are obtained; due to the artifacts induced by random cleavage operation, some stable pores appear to be missing in the centre part of the porous layer.[4] The diameters of stable pores are $\sim 1.5\,\mu$m, significantly larger than the top diameters (around 5–10 nm before KOH wet etching, cf. (a) and its caption). The etch rate is $\sim 4.6\,\mu$m/min. (c) Cross-section (magnification of (b)): The openings of macropores are formed by a nanoporous layer (cf. (a)), which can effectively serve as a diffusion barrier for chemical species.

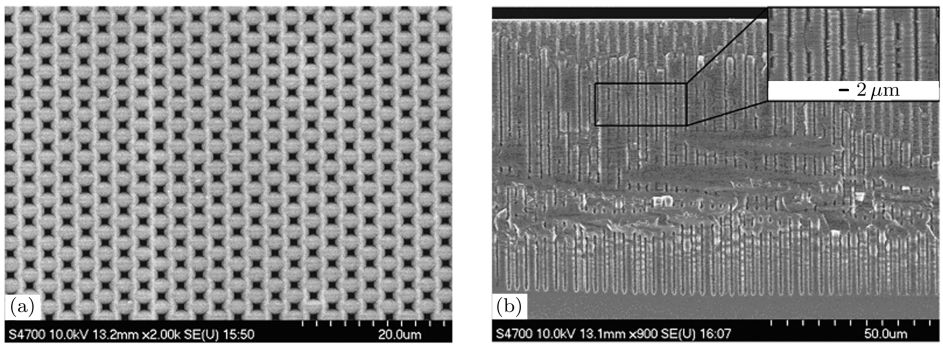


Fig.2. SEM micrographs: 40% HF, 140 W illumination, 18 V for 15 min, current density j (after 5 minutes of etching) $\approx 72\,\mathrm{mA/cm^2}$. (a) Plan-view: The pores are hexagonally arrayed. Top-diameters (around 0.7 μm) of pores show little variation over the anodized surface. (b) Cross-section (showing (011) plane): Stable pores with $\sim 95\mu$m depths and with $\sim 1\,\mu$m diameters are obtained; the pore sizes are apparently smaller than that of Fig.1(b) (where the bias, [HF] and illumination is the same as in this case). The etch rate is $\sim 6.3\,\mu$m/min.

4. Discussions

4.1. The analysis of current-voltage curves

To expose the bare relationship between initial surface morphology and electric field effect, the current-voltage ($I - V$)characteristics for 40% HF were measured on patterned and unpatterned samples in the dark (Fig.3). For the unpatterned sample (Curve B of Fig.3), starting from the open circuit potential (OCP), the current increases with increasing bias up to a plateau region which reveals the well-known hot carrier effects resulting from a strong field strength (10^3–10^5 V/cm). In this region, the current density slightly increases with increasing SCR width (corresponding to an enhanced potential) since the current is generated by carriers thermally activated via generation-recombination centre in SCR (Schottky barrier layer). No formation of 'breakdown' pores[24] can be expected across the whole scanned range of biases since for a planar Schottky junction of our highly resistive material (8–9 $\Omega \cdot$ cm), the pore formation potential (PFP) cannot be reached before 9 V.[25,43] By contrast, the pre-created defects exert a drastic influence upon the PFP (Curve A of Fig.3): the PFP, with which breakdown starts to occur, is around 0.3 V. The current corresponding to PFP is about 5–8 times the corresponding plateau current of Curve B and thus can only be interpreted as 'breakdown' current (current generated by electrical breakdown), just as pointed out by an existing report.[43] Note that after PFP, the current densities soar up to a rather high value, which can be a few decades greater than the plateau current of Curve B. This can be understood if considering the morphological difference of the two different kinds of samples: in our cases, the shape of the Schottky junctions of untextured and textured specimens can be respectively approximated to a plane and a semi-sphere with a radius around 5 nm (which can be largely identified by Fig.4).[25] According to Lehmann *et al*,[25] for equal bias, e.g., 0.3 V, the field strength around spherical tips of 5 nm radii can be enhanced to a value ($\sim 1.6 \times 10^6$ V/cm) significantly higher than that of a plane ($\sim 8 \times 10^3$ V/cm). This can explain why the PFP (at which breakdown occurs) in Fig.3 is ~ 0.3 V, since a 0.3 V bias (for spherical tips with 5 nm radii) can result in a field strength of 10^6 V/cm,[30] which can trigger a pronounced tunnelling breakdown. Therefore, the 'breakdown' current density (Curve A) can be much higher than the current density (Curve B) purely generated by thermal activation, as also pointed out in Ref.[43]. In addition, the $I - V$ curves measured for 10% HF exhibit the same global behaviour as the case of 40% HF except that the overall current density is lower due to a thinner HF (a lower [HF]). Hence, the field enhancing factors of different structures can be distinct from each other.

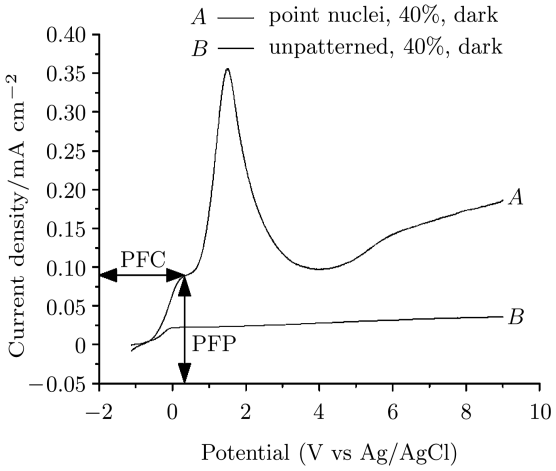


Fig.3. The current-voltage curves for 40% HF acquired in the dark with a scan rate of 30 mV/s. The potential is referred to Ag/AgCl electrode. The nitride mask on patterned samples has been removed before measurement. The peak value of A can be a few tens greater than the plateau current ($\sim 20\,\mu$A cm^{-2}) of B; the pore formation potential (PFP) is about 0.3 V, with the corresponding pore formation current (PFC) around 90 μA cm^{-2}.

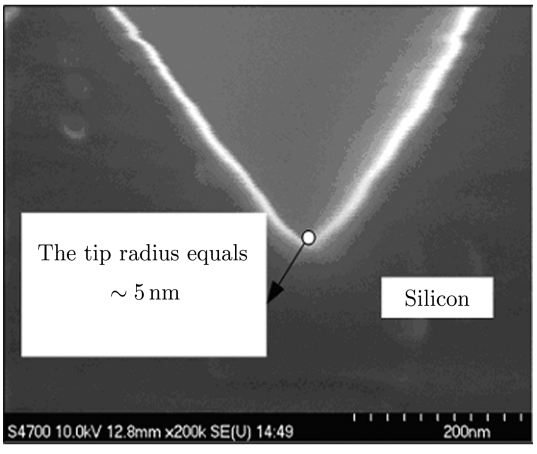


Fig.4. SEM micrograph (showing (110) plane): The actual tips of pre-structured defects show tip radii around a few nanometres. The artificial defect in this picture is formed with nitride mask by a prolonged TMAH etching to obtain structures as sharp as possible.

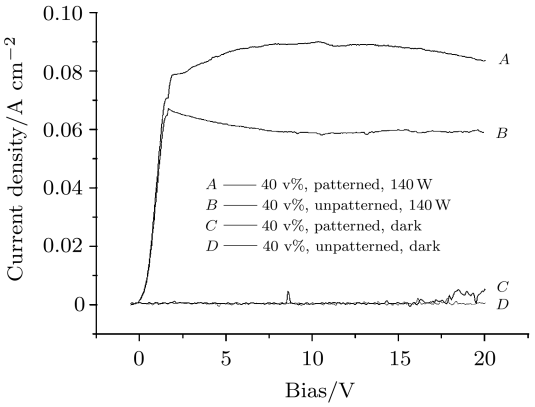


Fig.5. The $I-V$ curves A and B measured with illumination (140 W) but without pseudo-reference electrode. Curves C and D are measured in the dark for the comparison with curves A and B. The nitride mask on patterned samples has been removed before measurement. Compared with Fig.3, the scan rate is set to a quicker one (50 mV/s) due to a wider scan range (−0.5–20 V). Either for 10% or for 40% HF, the current density of patterned specimens is much higher than that of unpatterned ones.

The various correlations between field effects and different structures in our cases can be further displayed in Fig.5 (measured with illumination). Compared with planar substrates, due to a stronger field strength around sharp structures and thus a more efficient collection of minority carriers, the current density of textured specimens is higher than that of untextured samples. Additionally, in Fig.5 the ratio of photo-current to breakdown current is about 10–100 across the whole scanned range of biases (−0.5–20 V). Considering the actual bias 18 V in the experiments (Figs.1 and 2), the resulting photo-current (e.g., $\sim 50\,\mathrm{mA/cm^2}$ for unpatterned sample) can be about 2 orders of magnitude greater than the corresponding breakdown current (e.g., $\sim 0.4\,\mathrm{mA/cm^2}$ for unpatterned sample) as shown in Fig.5. Therefore the stable pores formed in our cases can be termed macropores,[40] showing a distinct difference from the so-called 'breakdown' mesopores.[24] Similarly, the local current density j_{tip} around stable-pore tips can be supposed to be approximate to j_{PS} and the dissolution valence (number of consumed carriers per etched silicon atom) n can be assumed to be ~ 2.7 (as pointed out in Refs.[2] and [24]), thus rendering the theoretical results in Table 1 fairly reasonable.

So, based on various field effects around different structures as analysed above and also the variation of physical and chemical parameters of patterned and unpatterned substrates, the diversity of deviation of observations from theory, seemingly incompatible but in fact unifiable, can be interpreted as follows.

4.2. The diversity of observations on patterned and unpatterned samples

Under the same etching condition, the size of stable pores (Fig.1) on the untextured substrate is much larger than that of the patterned specimen (Fig.2): diffusion barrier effects[32] originating from varied distributions of electric field around dissimilar structures at the start of each etching should be considered. In the case of unpatterned samples, the top diameter of pores is considerably smaller than that of patterned samples. This can be clearly visualized if we compare Fig.1(c) with Fig.2(a): the openings of stable pores in Fig.1(c) and Fig.2(a) are not in the same order of magnitude. Thus a much stronger diffusion barrier for chemical species of electrolytes can be expected in the case of Fig.1(c). This can reduce the [HF] in the pores more effectively and finally lead to a larger pore size resulting from a stronger oxidizing power of the thinner electrolyte in the pore, as can be deduced from CBM[29] and evidenced in our previous works.[44,45] That is, if the etching conditions (except [HF]) remain unchanged, the diameter of the pores is determined by chemistry factors and there is a negative correlation between [HF] and pore sizes.[29,44] Note that the potential drop in the pores can be neglected in our cases, since [HF] (40%) is rather high and it is known that for n-Si (n-type silicon) the applied potential drops predominantly across SCR even with a [HF] as low as 1%.[46]

On the other hand, the different sizes of pore openings in the two cases (either with or without predefined pattern) can only be correlated with a distinct surface morphology, since in our cases the unique variant is the initial physical status of the sample surface. This structural dissimilarity leads to a different field distribution beneath the surface, as described in subsection 4.1. Compared with unpatterned substrates, for an equal etching condition the prestructured nuclei on patterned samples can gather much more current bursts (CBs) and thus a larger opening can form in the pore-nucleation phase due to an inherently stochastic interaction of CBs, as stressed in CBM.[24] Then, due to the above-mentioned diffusion barrier effects, the actual [HF] beneath the opening of pores for the unpatterned case is always lower than that for the patterned one (in a given bulk electrolyte). This chemical

factor directly accounts for the different sizes of stable pores, but the origin of the difference in pore-size lies in physical factors, i.e., different field effects in the pore nucleation stage as discussed above. This supposition can be further corroborated by Fig.5: for a given [HF] the current density of patterned specimens is fairly higher than that of unpatterned ones, since for a given potential a larger pore opening (resulting from a greater electric field) and thus a thicker HF in the pores can be expected on textured samples. Note that under equal etching conditions, a thicker HF results in a higher current density. In summary, compared with unpatterned surface, a more pronounced field enhancement on patterned surface leads to a greater top diameter and finally to smaller stable pores due to a weaker diffusion barrier effect. Thus, for unpatterned sample (Fig.1), larger stable pores naturally result in a lower pore-density in comparison with patterned specimen (Fig.2). Likewise, a stronger diffusion barrier of unpatterned substrate leads to a thinner HF and hence to a slower etch rate than that of patterned substrate.

Generally, the fundamental reason rests on the variation of physical and chemical parameters of patterned and unpatterned substrates.

4.3. The deviation from SCR model

First, for the sake of clarity, SCR model will be briefly introduced here. Very regular macropore array was initially found by Lehmann and Föll in 1990,[1] but to date, some of the detailed formation mechanisms are still open to discussion.[41] As is well known, illuminating the back side of n-type silicon generates electron–hole pairs. The electrons are extracted by the back-side contact, whereas the holes (minority carriers in n-Si) diffuse from the back side through the wafer to the interface between silicon and electrolyte. Depending on silicon resisitivity and applied bias, an extended space charge region (SCR) evolves within the silicon. The overlapped SCR thus helps to passivate pore wall, while the bent SCR around pore-tips acts on the electronic holes and concentrates them mainly to the pore tips, promoting silicon dissolution there. Assuming a planar one-dimensional Schottky junction, Eq.(1) gives the SCR width d_{SCR}.

$$d_{\mathrm{SCR}} \approx \sqrt{2V_{\mathrm{Bias}}\varepsilon_{\mathrm{Si}}\varepsilon_0\mu_n\rho}, \tag{1}$$

where V_{Bias} is the applied bias, $\varepsilon_{\mathrm{Si}}$ and ε_0 are the dielectric constants of Si and vacuum permittivity, respectively; e is elementary charge, ρ the resistivity of Si and N_{d} the concentration of donors.

Based on the model of Lehmann,[2] the local current density around pore tips is always j_{PS}, thus justifying Eq.(2),

$$\frac{A_{\mathrm{pore}}}{A_{\mathrm{lattice}}} = \left(\frac{d}{a}\right)^2 = \frac{j}{j_{\mathrm{PS}}} \tag{2}$$

where j is the current density flowing across the silicon-electrolyte interface and j_{PS} is the critical current density determined by mass transfer of the electrolyte, and A_{pore} is the pore area, A_{lattice} the area of pore lattice, d the pore diameter and a the pore lattice constant.

For the same reason, since the local current density around pore tips is always assumed equal to j_{PS}, the etching speed ν thus does not depend on the global current density j.[2] Specifically,

$$\nu = \frac{j_{\mathrm{PS}}}{n(-e)N_{\mathrm{Si}}}, \tag{3}$$

where n is the dissolution valence (number of consumed carriers per dissolved silicon atom), e (1.602×10^{-19} C) the elementary charge and N_{Si} ($5 \times 10^{22}/\mathrm{cm}^3$) the atom density of silicon sample.

In our cases, for a known resistivity (8–9Ωcm) and bias (18 V), d_{SCR} equals $\sim 4.2\,\mu$m, according to Eq.(1). In Table 1, the theoretical values were obtained based on the known current density j (recorded after 5 minutes of etching, cf. Section 3). Meanwhile, according to Eq.(2), $d = a\sqrt{j/j_{\mathrm{PS}}}$ and theoretical pore diameter can be obtained, since j_{PS} equals $\sim 983\,\mathrm{mA\ cm}^{-2}$ for our cases and can be calculated from an equation in Ref.[2], and a is supposed to equal $4d_{\mathrm{SCR}}$ (according to SCR effects).[2] Note that the volume percentage of HF has been converted into weight percentage, e.g., for the calculation of j_{PS}. Similarly, according to the equation $p \approx 1/(16d_{\mathrm{SCR}}^2)$,[2] the theoretical pore density p can be obtained as $\sim 0.0035\,\mu\mathrm{m}^{-2}$ and thus is approximately 10–35 times lower than the empirical results (see the third column of Table 1). As pointed out in the SCR model, the local current density j_{tip} around pore tips in our case can be approximate to j_{PS}, due to a high ratio (> 10) of photo-current to breakdown-current as is implied in Fig.5, and thus the dissolution valence equals ~ 2.7.[2,24] Therefore, theoretical etch rate ν can be calculated from Eq.(3). If based on the j (observed after 5 minutes of etching as stated above), the value of n (calculated via gravimetry according to the

formula of n[47]) is ~ 2.54 and accords largely with the reported one (~ 2.7).[2,24] Therefore the theoretical etch-rate 21.9 μm min^{-1} based on a dissolution valence of 2.54 is approximate to the corresponding value (20.8 μm min^{-1}) in Table 1, still rendering our conclusion (given in Section 3) justifiable. Note that under a constant-voltage condition in our cases, it is hard to determine the precise value of n since the current densities are ever-changing; for the same reason, the local current density $j_{\rm tip}$ around pore tips can hardly be precisely acquired and thus was assumed to be approximate to $j_{\rm PS}$.[2,24] Also, it should be noted that in Table 1 the results of theoretical calculation were in light of SCR principles by assuming $a \approx d_{\rm SCR}$, that is, no modification was made as advised in Ref.[5]. If introducing modification in accordance with $a \approx 2d_{\rm SCR}$,[5] the calculated pore density, four times the corresponding one presented in Table 1, will be 3–8 times lower than the observed results (cf. Rows 1 and 2 of Table 1), which still differ considerably from the theoretical prediction.

Generally, the results achieved here (Figs.1 and 2) cannot be readily interpreted by SCR model: the bias applied (18 V) was one order of magnitude above the voltage ($\sim$1.5 V) determined by SCR principles. Note that the SCR width ($\sim 4.2\,\mu$m) is larger than the actual pore distance (e.g., 3 μm in Fig.2). Hence, it has to be pointed out that the overall results dissent from SCR principles: the underlying reason (a qualitative interpretation) can be found elsewhere.[40]

5. Conclusions

The change of pore size, pore density and pore etch-rate on patterned and unpatterned samples were evidenced. Based on the analysis of SEM micrographs and $I-V$ curves, the varied electric-field effects as well as current-burst-model were employed to interpret the underlying mechanism; the variation of physical and chemical parameters induced by the difference in original morphology of sample surface was finally found to be crucial for understanding the observations. Additionally, our observation deviates from SCR principles.

References

[1] Lehmann V and Föll H 1990 *J. Electrochem. Soc.* **137** 653
[2] Lehmann V 1993 *J. Electrochem. Soc.* **140** 2836
[3] Lehmann V 1995 *Thin Solid Films* **255** 1
[4] Lehmann V and Grüning U 1997 *Thin Solid Films* **297** 13
[5] Rifai M H A, Christophersen M, Ottow S, Carstensen J and Föll H 2000 *J. Electrochem. Soc.* **147** 627
[6] Lehmann V and Rönnebeck S 1999 *J. Electrochem. Soc.* **146** 2968
[7] Propst E K and Kohl P A 1994 *J. Electrochem. Soc.* **141** 1006
[8] Searson P C, Macaulay J M and Prokes S M 1992 *J. Electrochem. Soc.* **139** 3373
[9] Allongue P, Costa-Kieling V and Gerischer H 1993 *J. Electrochem. Soc.* **140** 1009
[10] Allongue P, Villeneuve C, Pinsard L and Bernard M 1995 *Appl. Phys. Lett.* **67** 941
[11] Theunissen M J J 1972 *J. Electrochem. Soc.* **119** 351
[12] Beale M I J, Benjamin J D and Uren M J 1985 *J. Cryst. Growth* **73** 622
[13] Smith R L, Chuang S F and Collins S D 1988 *J. Electron. Mater.* **17** 533
[14] Smith R L and Collins S D 1992 *J. Appl. Phys.* **71** R1
[15] Kang Y and Jorne J 1993 *J. Electrochem. Soc.* **140** 2258
[16] Parkhutik V P 1994 *Porous Silicon World Scientific* p301
[17] Valance A 1995 *Phys. Rev.* B **52** 8323
[18] Carstensen J, Christophersen M and Föll H 2000 *Mat. Sci. Eng.* B **69–70** 23
[19] Claussen J C, Carstensen J, Christophersen M, Langa S and Föll H 2003 *Chaos* **13** 217
[20] Zhang X G 2004 *J. Electrochem. Soc.* **151** C69
[21] Zhang X G 2001 *Electrochemistry of Silicon and Its Oxides* (Norwell, MA: Kluwer) p312
[22] Lust S and Levy-Clement C 2002 *J. Electrochem. Soc.* **149** C338
[23] Zhang X G, Collins S D and Smith R L 1989 *J. Electrochem. Soc.* **136** 1561
[24] Föll H, Christophersen M, Carstensen J and Hasse G 2002 *Mat. Sci. Eng.* R **39** 93
[25] Lehmann V, Stengl R and Luigart A 2000 *Mat. Sci. Eng.* B **69–70** 11
[26] Matthias S, Müller F, Schilling J and Gösele U 2005 *Appl. Phys.* A **80** 1391
[27] Levy-clement C, Lagouby A and Tomkiewicz M 1994 *J. Electrochem. Soc.* **141** 958
[28] Wehrspohn R B, Ozanan F and Chazalviel J N 1999 *J. Electrochem. Soc.* **146** 3309
[29] Christophersen M, Carstensen J and Föll H 2000 *Phys. Status Solidi* (a) **182** 45
[30] Searson P C, Macaulay J M and Ross F M 1992 *J. Appl. Phys.* **72** 253
[31] Föll H, Langa S, Carstensen J, Christophersen M and Tiginyanu I M 2003 *Adv. Mater.* **15** 183
[32] Frey S, Kemell M, Carstensen J, Langa S and Föll H 2005 *Phys. Status Solidi* (a) **202** 1369
[33] Föll H, Carstensen J and Frey S 2006 *J. Nanomater.* **2006** 1
[34] Langa S, Tiginyanu I M, Carstensen J, Christophersen M and Föll H 2003 *Appl. Phys. Lett.* **82** 278

[35] Chen Y, Wang L W and Sarro P M *Highly controllable electrochemical deep etching process on silicon* MEMS 2005 30 Jan.–3 Feb. p512 doi:10.1109/MEMSYS.2005.1453979
[36] Wang Z, Wang L W, Nguyen N T, Wien W A H, Schellevis H, Sarro P M and Burghartz J N 2006 *IEEE Trans. on Advanced Packaging* **29** 615
[37] Kan P Y Y and Finstad T G 2007 *Thin Solid Films* **515** 5241
[38] Bhagavannarayana G, Sharma S N, Sharma R K and Lakshmikumar S T 2006 *Mater. Chem. Phys.* **97** 442
[39] Bao X Q, Jiao J W, Wang Y L, Zhang Y, Ge D H, Na K W and Choi H 2007 *Electrochem. Commun.* **9** 1491
[40] Bao X Q, Lin J L, Jiao J W and Wang Y L 2007 *Electrochim. Acta* **53** 823
[41] Bao X Q, Jiao J W, Duan F, Wang Y L, Na K W and Choi H 2007 *Electrochem. Commun.* **9** 1689
[42] Ohji H 2002 *Macroporous Si based micromachining* (Ph.D. thesis, Delft, the Netherlands) pp90-51, pp66-90
[43] Schmuki P, Erikson L E and Lockwood D J 1998 *Phys. Rev. Lett.* **80** 4060
[44] Bao X Q, Jiao J W, Wang Y L, Na K W and Choi H 2007 *J. Electrochem. Soc.* **154** D175
[45] Bao X Q, Jiao J W, Zhou J and Wang Y L 2007 *Electrochim. Acta* **52** 6728
[46] Searson P C and Zhang X G 1990 *J. Electrochem. Soc.* **137** 2539
[47] Christophersen M, Carstensen J, Ronnebeck S, Jager C, Jager W and Föll H 2001 *J. Electrochem. Soc.* **148** E267